Biochimica et Biophysica Acta 1827 (2013) 348–354

Contents lists available at SciVerse ScienceDirect

Biochimica et Biophysica Acta

journal homepage: www.elsevier.com/locate/bbabio

Characterization of the *Synechocystis* PCC 6803 Fluorescence Recovery Protein involved in photoprotection

Michal Gwizdala, Adjélé Wilson, Amin Omairi-Nasser, Diana Kirilovsky *

Commissariat à l'Energie Atomique (CEA), Institut de Biologie et Technologies de Saclay (iBiTec-S), 91191 Gif sur Yvette, France
Centre National de la Recherche Scientifique (CNRS), UMR 8221, 91191 Gif sur Yvette, France

ARTICLE INFO

Article history:
Received 24 September 2012
Received in revised form 31 October 2012
Accepted 6 November 2012
Available online 15 November 2012

Keywords:
Cyanobacteria
Orange Carotenoid Protein
Non-photochemical quenching
Photoprotection
Photosynthesis
Phycobilisome

ABSTRACT

Under high irradiance, most cyanobacteria induce a photoprotective mechanism that decreases the energy arriving at the photosynthetic reaction centers to avoid the formation of dangerous species of oxygen. This mechanism which rapidly increases the heat dissipation of excess energy at the level of the cyanobacterial antenna, the phycobilisomes, is triggered by the photoactivation of the Orange Carotenoid Protein (OCP). Under low light conditions, the Fluorescence Recovery Protein (FRP) mediates the recovery of the full antenna capacity by accelerating the deactivation of the OCP. Several FRP *Synechocystis* mutants were constructed and characterized in terms of the OCP-related photoprotective mechanism. Our results demonstrate that *Synechocystis* FRP starts at Met26 and not at Met1 (according to notation in Cyanobase) as was previously suggested. Moreover, changes in the genomic region upstream the ATG encoding for Met26 influenced the concentration of OCP in cells. A long FRP (beginning at Met1) is synthesized in *Synechocystis* cells when the *frp* gene is under the control of the *psbA2* promoter but it is less active than the shorter protein. Overexpression of the short *frp* gene in *Synechocystis* enabled short FRP isolation from the soluble fraction. However, the high concentration of FRP in this mutant inhibited the induction of the photoprotective mechanism by decreasing the concentration of the activated OCP. Therefore, the amplitude of photoprotection depends on not only OCP concentration but also on that of FRP. The synthesis of FRP and OCP must be strictly regulated to maintain a low FRP to OCP ratio to allow efficient photoprotection.

1. Introduction

Photosynthetic organisms are exposed to fluctuating light conditions. The ability of these organisms to adapt themselves to these changing conditions determines their survival and their evolutionary success. One mechanism of adaptation and photoprotection regulates the energy arriving at the reaction centers. Under low light conditions, the energy-collecting antennae efficiently funnel the absorbed light energy into the reaction centers. Under high light conditions, changes in the antennae are induced and the excess absorbed energy is dissipated as heat instead of being transferred to the reaction centers. This decreases the generation of reactive oxygen species, which are destructive for the photosynthetic apparatus and potentially lethal for the organism itself.

The molecular mechanisms involved in antenna-related photoprotection are different in plants and cyanobacteria. The antenna of higher plants and green algae are membrane embedded chlorophyll- and carotenoid-binding protein complexes (reviewed in [1]) that upon sensing the acidification of the lumen of the thylakoids, switch from an energy funneling- into an energy dissipating-mode (last reviewed in [2,3]). In cyanobacteria, the antenna, called phycobilisome (PB) is an extra-membrane complex formed by proteins, which covalently bind blue and red bilins, the phycobiliproteins. The PBs which are attached to the stromal side of the thylakoid membrane, are formed by a core, from which six rods radiate. Both core and rods are composed of phycobiliproteins connected by linker proteins tuning the spectral properties of the pigments to ensure efficient excitation-energy transfer to the reaction centers (reviewed in [4–7]). The rods are composed of hexamers of phycocyanin (PC) emitting at 650 nm and the core is built of trimers of allophycocyanine (APC) emitting at 660 and 680 nm. In most cyanobacteria, strong blue-green light induces an increase of heat dissipation of the absorbed energy at the level of the core of the PBs [8–11]. However, PBs alone are not capable of performing this functional switch; they need to interact with a soluble carotenoid protein, the Orange Carotenoid Protein (OCP) [10].

The OCP, a ubiquitous protein of 35 kDa, carries a keto-carotenoid, 3′-hydroxyechinenone, in an all-trans conformation. The protein has two domains: the all-α-helical N-terminal domain and the mixed α-helical/β-sheet C-terminal domain. The carotenoid spans both domains [12–14]. The OCP is photoactive: in darkness or low light it appears orange (OCP^o); strong blue-green light triggers conformational changes of the carotenoid and the protein. Upon photoactivation, the

* Corresponding author at: iBiTec-S, Bât 532, CEA Saclay, 91191 Gif sur Yvette, France. Tel.: +33 1 69089571; fax: +33 1 69088717.
E-mail address: diana.kirilovsky@cea.fr (D. Kirilovsky).

0005-2728/$ – see front matter © 2012 Elsevier B.V. All rights reserved.
http://dx.doi.org/10.1016/j.bbabio.2012.11.001

metastable red form of OCP (OCP^r) accumulates [15]. In darkness, OCP^r reconverts to OCP^o. The kinetics of reconversion is strongly temperature dependent. OCP^r is stabilized at lower temperatures [15].

Only OCP^r is able to bind to the core of PBs to induce an increase of thermal energy dissipation [15–17]. The increase of thermal dissipation is accompanied by a simultaneous decrease of PB fluorescence and of energy transfer from PB to reaction centers. In vitro, OCP^r forms a stable complex with PB and this binding is almost irreversible [17]. However, in vivo, the "quenched" cells, when transferred to darkness or dim light, recover in minutes the lost fluorescence (and the full capacity of the antenna), suggesting the detachment of the OCP from PB. The in vivo recovery needs another protein, the Fluorescence Recovery Protein (FRP). Mutants missing this protein, once quenched, only partially recover the full capacity of antenna [18]. In vitro, when FRP is added to the quenched OCP–PB complexes, it induces the recovery of fluorescence and the detachment of OCP from the PB [17]. Thus, FRP is an off-switch of the OCP-mediated photoprotection [17,18]. In *Synechocystis*, the FRP is encoded by the *slr1964* gene. In fresh water cyanobacteria strains (including *Synechocystis*) the *frp* gene is downstream the *ocp* gene. In marine strains a β-carotene ketolase-encoding gene is in-between these two genes [18]. The FRP is a non-chromophorylated soluble protein of unknown structure. Its theoretical mass is around 13 kDa [18,19]. It interacts only with the red form of OCP and greatly accelerates its reconversion to the orange form [18].

FRP contains between 106 and 111 amino acids in most of the sequenced cyanobacteria strains [18]. Only the FRPs of *Mycrocystis* NIES 843 and *Synechocystis* seem to be longer based on Cyanobase.org data. In both strains, the FRP contains an N-terminal prolongation of 22 to 25 amino acids. In *Synechocystis*, this additional sequence contains four ATG or GTG codons. The first GTG is considered as the first Met (Cyanobase numeration) of the FRP. The fourth Met (Met26) coincides with the first Met of most of homologues [18]. In the past, we have constructed a *Synechocystis* mutant in which the *frp* gene beginning in the GTG encoding for Met1 was under the control of the *psbA* promoter [18]. This strain produced relative high concentrations of an active "long" FRP but all attempts to isolate an active FRP starting at Met1 were unsuccessful [18]. The long FRP remained strongly attached to the membrane and the detergent, which was needed to isolate it, affected its activity. When this cyanobacterial gene was overexpressed in *Escherichia coli* the protein was isolated as inclusion bodies. Denaturation and renaturation, of these inclusion bodies to obtain an active protein, were fruitless. In contrast, a shorter version of the gene encoding for a FRP starting at Met26 was successfully overexpressed in *E. coli* and the corresponding protein was isolated in a soluble and active form [18]. In the in vitro studies described in Boulay et al. [18] and Gwizdala et al. [17] this short version of FRP (short FRP) was used.

Based on our past results, a doubt appeared about the real length of the *Synechocystis* FRP and the first Met of the protein. In this work, we have constructed a series of *Synechocystis* mutants to compare the activity and characteristics of the "short" and "long" FRPs in vivo and to elucidate the presence or absence of the N-terminal prolongation in the *Synechocystis* WT FRP. One of these mutants allowed the isolation of the "short" FRP from *Synechocystis* cells and its characterization. In addition, the study of mutations introduced between the *ocp* and *frp* genes gave us some information about the regulation of OCP synthesis.

2. Material and methods

2.1. Construction of FRP mutants

A summary of the genotypes and names of the mutants used in this work is described in Fig. 1 and the details of the different constructions are described in Figures S1, S2 and Table S1.

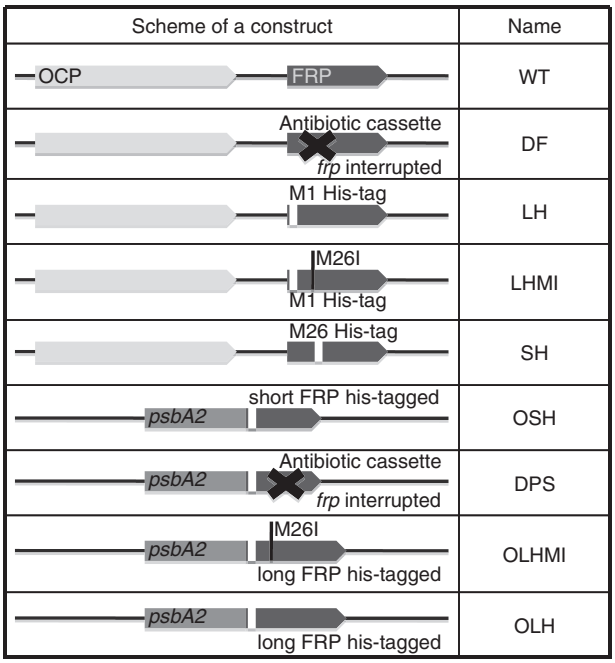

Fig. 1. Constructs used in this study. The *ocp* gene is marked with light gray and the *frp* gene in dark gray. The symbol X in the *frp* gene stands for an antibiotic resistance cassette; the white bar indicates the position of the His-tag and the black line indicates the presence of the M26I point mutation. The "*psbA2*" is the promoter of the *psbA2* gene that was used as a strong promoter to overexpress the *frp* gene. Names of mutants used in this article are in the second column. Details in Figure S1 and S2. Mutants DF and OLH were described in Boulay et al. [18].

A 2.2 kb fragment containing the *slr1963* (encoding for OCP) and *slr1964* (encoding for FRP) genes was amplified by PCR from the *Synechocystis* PCC 6803 genome using restriction sites-creating primers car7XhoI and car6SpeI (Table S1). This fragment was cloned into the SK (+) ampicillin-resistant vector. A BamHI restriction site was created downstream the end of the *slr1964* gene by site-directed mutagenesis (Table S1). A 2000 bp spectinomycin and streptomycin resistance cassette with a transcription terminator was then inserted into the unique restriction site BamHI of the plasmid (Fig S1). His_6-Tag was added after the ATG encoding for the Met1 or the Met26 in the *slr1964* gene in this plasmid. To construct the N-terminal His_6-tagged M26I-FRP, a point mutation was introduced in the *slr1964* gene by site-directed mutagenesis. All plasmids were checked by sequencing and used to transform wild-type *Synechocystis* PCC 6803 cells. Complete segregation was tested by PCR amplification.

2.2. Overexpression of the long or the short His-tagged frp in Synechocystis

To obtain a strain overexpressing a N-terminal His_6-tagged long *frp* (M26I) or short His-tagged *frp*, a plasmid containing the long *slr1964* gene under the control of the *psbA2* promoter was used (Fig S2). The construction of this plasmid and the strain which overexpress a N-terminal His_6-tagged *frp* were described in [18]. The point mutation M26I or the deletion of the nucleotides coding for the first 25 amino-acids (short FRP) was introduced in the *slr1964* gene in the overexpressing plasmid by site-directed mutagenesis using the Quickchange XL site-directed mutagenesis kit (Stratagene) and synthetic primers (Table S1). The presence of the deletion or that of the point mutation was confirmed by DNA sequencing. These plasmids were used to transform the kanamycin resistant ΔFRP mutant of *Synechocystis* PCC 6803 [18].

To remove the short FRP sequence, a plasmid where the *psbA2* coding region was replaced by a 1.1 kb p-chloramphenicol resistance cassette was used to transform, the overexpressing short *frp* strain.

2.3. Overexpression of the short His-tagged frp in E. coli

To overexpress short His-tagged *frp* without thrombin in *E. coli*, the *slr1964* gene (beginning in the ATG coding for M26) was amplified by PCR using the petM26HISfor/petM26HISrev oligonucleotides (Table S1) and the pCB9 plasmid as template. The construction of the pCB9 plasmid was described in [18]. The ultracompetent XL10-gold strain (Stratagene) was transformed with this plasmid. Then, the plasmid was extracted and used for the transformation of the BL21 strain (Stratagene) adapted for gene overexpression. The plasmid was checked by sequencing. Primers used in this work are listed in Table S1.

2.4. OCP purification

OCP was isolated from the overexpressing C-terminal His-tagged OCP −ΔCrtR strain [20]. Its purification was performed as previously described [15].

2.5. Purification of the FRP from E. coli and the Synechocystis overexpressing short His-tagged frp (OSH)

The isolation of the FRP from the E. coli strain overexpressing the His-tagged short FRP of Synechocystis was described in (18).

Synechocystis OSH mutant cells (1 mg Chl mL^{-1}) were broken in 100 mM Tris–HCl pH 8.0 using a French Press. The membranes were pelleted and the supernatant was loaded on a column of Ni-ProBond resin (Invitrogen). The FRP was eluted with 300 mM imidazol and dialyzed during 48 h against 40 mM Tris–HCl at pH 8.0. Further purification was performed on a Whatman DE-52 cellulose column. The FRP was eluted with 80 mM NaCl in 40 mM Tris–HCl and dialyzed overnight against 40 mM Tris–HCl at pH 8.0. Purity of FRP was checked by SDS–PAGE, on a 17% polyacrylamide/2 M urea in a TRIS/MES system [21].

2.6. Fluorescence measurements

Fluorescence quenching and recovery were monitored with a pulse amplitude modulated fluorometer (101/102/103-PAM; Walz, Effelrich, Germany). All measurements were carried out in a stirred cuvette of 1 cm diameter at 30 °C. The fluorescence quenching was induced by 870 μmol photons m^{-2} s^{-1} of blue-green light (400–550 nm). Recovery of fluorescence was recorded under dim blue-green light conditions (40 μmol photons m^{-2} s^{-1}).

2.7. Absorbance measurements

Cell absorbance was monitored with an UVIKONXL spectrophotometer (SECOMAN, Alès). Chl content was determined in methanol using the extinction coefficient at 665 nm of 79.24 mg mL^{-1} cm^{-1}. The orange to red photoconversion of the OCP was monitored in a Specord S600 (AnalyticJena, France) spectrophotometer during illumination with 5000 μmol photons m^{-2} s^{-1} of white light at 10 °C.

2.8. OCP and FRP Immunoblot detection

The quantity of OCP and FRP protein was analyzed by SDS–PAGE on a 12% or 17% respectively, polyacrylamide/2 M urea in a TRIS/MES system [21]. The OCP and the FRP proteins were detected by a polyclonal antibody against OCP and FRP respectively. Binding of antibodies was monitored by an alkaline phosphatase colorometric reaction (Biorad, AP Conjugate Substrate Kit) or by peroxidise chemiluminescence reaction (GE Healthcare, Amersham, ECL Prime Western Blotting Detection Reagent) (Figs. 5 and 7). Chemiluminesence was recorded with cooled CCD camera (DNR MicroChemi Bio Imaging System, GelCapture) and analyzed with ImageJ software. The detection was performed in membrane-bound phycobilisomes (MP) fractions obtained as previously described in [10].

3. Results

3.1. Characterization of Synechocystis strains overexpressing the long or the short frp gene

In order to compare the activities and characteristics of the "long" and the "short" FRPs, two mutants were constructed. In both mutants, the *frp* gene in its locus was interrupted and the *psbA2* gene was replaced by the long or short *frp* gene. In these mutants the *psbA2* gene is absent but it was previously shown that deletion of this gene does not result in any modification in the strong blue-green light induced fluorescence quenching and/or in the recovery [18]. In the OLHMI mutant, the *frp* gene starting at the GTG coding for Met1 and containing a mutation that leads to the replacement of Met 26 by an Ile was under the control of the *psbA* promoter. The mutation at Met26 was introduced to be sure that no short FRP is present in this mutant. In the OSH mutant, the *frp* gene starting at the fourth ATG encoding for Met26 was under the control of the *psbA* promoter. An N-terminal His-tag was introduced in the short and the long FRPs in order to detect the proteins. Our anti-FRP antibody, which was obtained using a denatured N-terminal His-tagged long FRP isolated from *E. coli* inclusion bodies, detects only the short or the long FRP containing an N-terminal His-tag [18]. The WT FRP and a His-tagged C-terminal FRP are not detected by this antibody [18]. However, it is specific for FRP since it does not recognize the His-tagged OCP [18].

We first compared the OLHMI mutant to a previously constructed "over-FRP" mutant, in which the long *frp* gene (beginning in the GTG encoding for Met1) without the M26I point mutation, was under the control of the *psbA* promoter (OLH mutant) [18]. The Western-blot in Fig. 2A shows that the size (about 13 kDa) and the quantity of FRP present in the cells and the membranes of both mutants were identical. No smaller band was detected. All long FRPs present in the cells were in the membrane fraction (Fig. 2A) as expected from previously published results [18]. The kinetics of fluorescence decrease under strong blue-green light (Fig. 3A) and those of fluorescence recovery

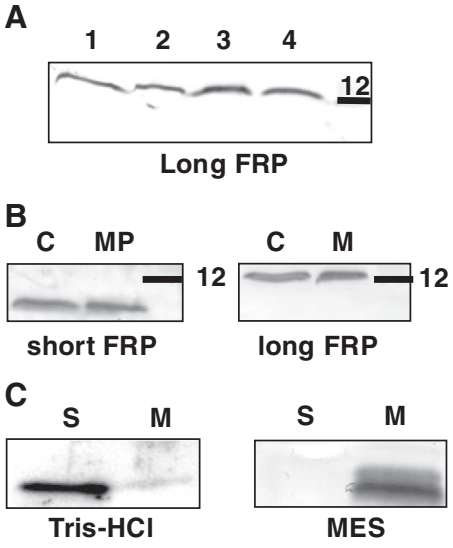

Fig. 2. Immunoblot detection of short and long FRP. (A) Immunoblot detection of long FRP in cells (1, 2) and in membranes (3, 4) of OLH (1, 3) and OLHMI (2, 4). (B) Immunodetection of short and long FRP in cells and MP fractions isolated from OSH and OLH cells respectively. (C) Immunodetection of short FRP in soluble (S) and membrane (M) fractions from OSH mutant cells broken in Tris–HCl (pH 8) or MES (pH 6). In A and B each lane contains 4 μg chlorophyll. In C each lane contains 40 μg protein.

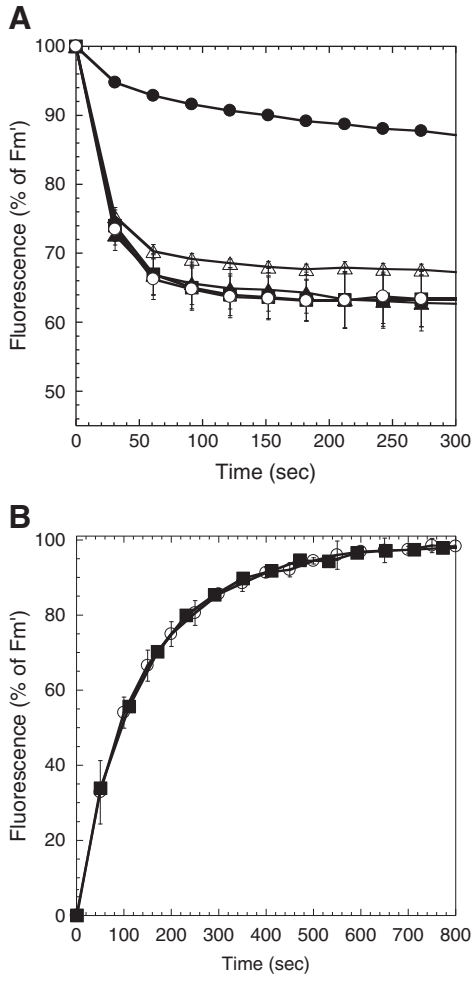

Fig. 3. Induction and recovery of the photoprotective mechanism by strong blue-green light in strains overexpressing the long or the short FRP. (A) Decrease of maximal fluorescence (Fm') during exposure to 870 μmol photons m^{-2} s^{-1} of cells of: WT (closed triangles), OLHMI (closed square), DPS (open triangles) and OSH (closed circles) and OLH (open circle). (B) Increase of maximal fluorescence (Fm') at 40 μmol photons m^{-2} s^{-1} in pre-quenched cells of: OLH (open circle) and OLHMI (closed square). Measurements at cell concentration of 3 μg Chl/mL and at 30 °C. Average of three independent experiments. Error bars represent SD.

(Fig. 3B) were also similar in both mutants. These results indicated that the M26I mutation does not inactivate the long FRP and that the OLH mutant only contains the long FRP. The presence of short FRP in this mutant in addition to the long FRP would result in a faster recovery. Thus, under the control of the *psbA2* promoter only the long version of the protein is synthesized in the presence or absence of Met26.

When OSH cells, overexpressing the short *frp*, were illuminated with strong blue-green light less than 10% of fluorescence quenching was induced while 30–35% of fluorescence quenching was observed in the strains overexpressing the long *frp* (OLH and OLHMI) (Fig. 3A). In the OSH mutant, the lost fluorescence recovered in less than 1 min. To confirm that the low level of fluorescence quenching was only related to the overexpression of the short *frp* another mutant was constructed. We re-transformed the OSH cells with a plasmid in which the short *frp* gene under the control of the *psbA2* promoter was replaced by an antibiotic resistance cassette. In the new mutant (DPS), strong blue–green light induced about 30% of fluorescence quenching like in WT cells (Fig. 3A). This result confirmed the relationship between very low fluorescence quenching and overexpression of the short *frp* gene in OSH mutant cells. In vitro experiments have already shown that the presence of relative low concentrations of FRP during illumination destabilizes OCP^r and decrease or inhibits its accumulation [17]. Under these conditions less fluorescence quenching was observed.

Our results also indicate that the short FRP has higher activity than the long FRP. The overexpression of the short *frp* inhibited the accumulation of OCP^r and the induction of fluorescence quenching. This was not observed when the long *frp* was overexpressed in OLH and OLHMI mutants. In addition, the fluorescence recovery was faster in the OSH than in the OLHMI and OLH mutants. The amount of FRP was similar in OSH and OLHMI cells (Fig. 2B).

We have already shown that the long FRP has a very strong interaction with the membrane. It was always present in the membrane fraction and salt washes were unable to detach the protein from the membrane [18]. The behavior of the short FRP was different. Fig. 2C shows that the short FRP was mostly in the soluble fraction when the cells were broken in 100 mM Tris–HCl (pH 8.0) but it remained attached to the membrane when the cells were broken in MES buffer (pH 6.0). This behavior was also observed for the OCP, which is found in the membrane fraction when the cells are broken in MES but it is present in the soluble fraction when the cells are broken in Tris–HCl [10,15]. The presence of the short FRP in the soluble fraction enabled the purification of the *Synechocystis* FRP (FRP^{syn}) from OSH mutant cells.

To isolate the short OCP, the OSH cells were broken in 100 mM Tris–HCl (pH 8.0) and the soluble fraction was loaded on a column of Ni-ProBond resin (Invitrogen). We eluted the FRP with 300 mM Imidazol. The FRP was further purified using a Whatman DE-52 cellulose column. The FRP^{syn} purity was confirmed by SDS–Page (Fig. S4).

The activity of FRP^{syn} was tested in vitro by measuring the kinetics of OCP^r to OCP^o dark conversion in the absence or presence of FRP^{syn}. Its activity was compared to that of the short FRP isolated from *E. coli* (FRP^{ec}) [18]. The OCP^o was first illuminated to convert it to OCP^r and then incubated in darkness in the presence of FRP^{ec} or FRP^{syn}. The dark reconversion to OCP^o was monitored with a spectrophotometer (Specord S600 AnalyticJena) at 10 °C (Fig. 4). In these conditions, in the absence of FRP the conversion OCP^r to OCP^o was very slow. After 15 min only 20% of OCP^r was converted to OCP^o. The presence of both of FRPs, FRP^{syn} or FRP^{ec}, largely accelerated this conversion. No differences in kinetics of reconversion were observed in presence of FRP^{ec} or FRP^{syn}. One FRP per 10 OCPs induced full reconversion with a $t_{1/2}$ of 200 s. By increasing the FRP to OCP molar ratio the kinetics were even faster. At 1 FRP per 2 OCPs the $t_{1/2}$ was 40 s. Thus, the activities of the short his-tagged FRPs isolated from *E. coli* and *Synechocystis* cells were similar.

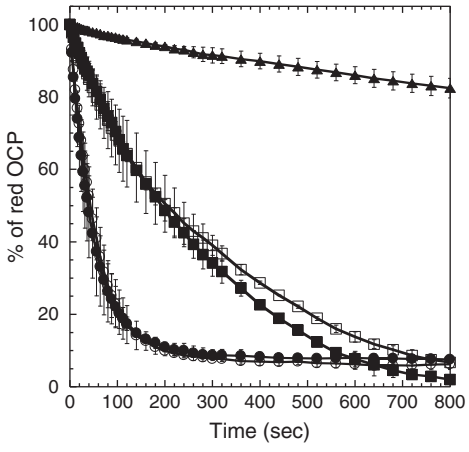

Fig. 4. Kinetics of dark reconversion OCP^r-to-OCP^o at 10 °C in the absence and the presence of FRP: without FRP (triangles), with 1 FRP per 10 OCPs (squares) and 1 FRP per 2 OCPs (circles) (molar ratios). Open symbols for *Synechocytsis* FRP, closed symbols for *E. coli* FRP. Average of three independent experiments. Error bars represent SD.

3.2. Synechocystis FRP begins at Met1 or at Met26?

Due to the high activity of the short FRP (higher than that of the long FRP) and to the fact that only *Synechocystis* and *Mycrocystis* FRPs seemed to have an N-terminal prolongation, big doubts appeared, concerning the real size of the WT *Synechocystis* FRP. In order to elucidate the presence or absence of the N-terminal prolongation two other mutants were constructed. A sequence encoding for 6 Histidines was introduced downstream the GTG encoding for Met1 (LH mutant) or the ATG coding for Met26 (SH mutant) of the *frp* gene in its locus to facilitate the detection of the FRP. In another mutant (LHMI), Met26 was replaced by an Ile to eliminate a possible translation starting site at Met26. In this mutant, which contains also a His-tag downstream Met1, only the long FRP could be present. In the LH mutant, a His-tagged long FRP or a non-His-tagged short FRP can be present. A previously constructed mutant lacking the FRP was also used in this study [15]. In this mutant the *frp* gene was interrupted by a kanamycin resistance cassette (DF mutant).

To study the influence of the *frp* mutations on fluorescence recovery kinetics, WT and mutant *Synechocystis* cells were preilluminated with strong blue-green light (870 μmol photons m^{-2} s^{-1}, 400–550 nm) for 2 min to induce fluorescence quenching and then they were incubated in dim blue-green light and the increase of fluorescence yield was followed with a PAM fluorometer (Fig. 5A). The WT and the SH (carrying a His-tag after Met26) and LH (carrying a His-tag after Met1) mutants recovered the fluorescence rapidly and almost completely within 10 min (Fig. 5A) indicating the presence of active FRPs in the mutants and WT. Although the concentration of short FRP is very low in SH cells we could detected its presence by Western-blot (Fig. 5B). However, we were unable to detect any traces of long FRP in the LH mutant (Fig. 5B) indicating the absence of long His-tagged FRP in this mutant. Since this mutant recovered the lost fluorescence, we concluded that in the LH mutant a short FRP beginning at Met26 is present, like in WT and SH cells. This short FRP was not detectable due to the lack of an N-terminal His-tag.

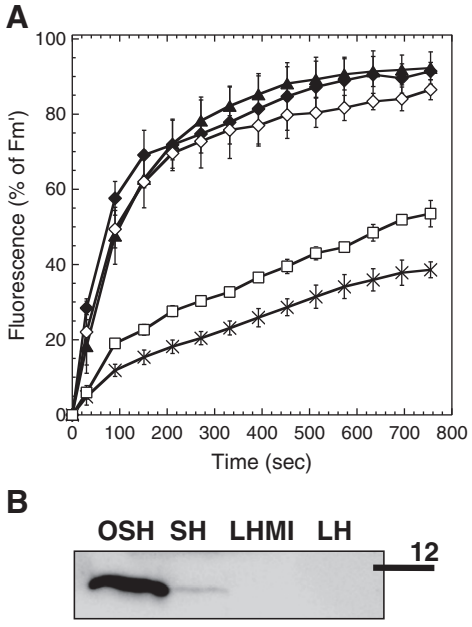

Fig. 5. (A) Recovery of fluorescence during exposure to dim blue-green light (400–550 nm) after 2 min of high irradiance at 30 °C. Increase of maximal fluorescence (Fm') at 40 μmol photons m^{-2} s^{-1} in pre-quenched cells of: WT (closed triangles), DF (crosses), SH (closed rhomboids), LH (open rhomboids) and LHMI (open squares). The cells were diluted to 3 μg Chl/mL. Average of three independent experiments. Error bars represent SD. (B) Immunoblot detection of FRP in MP isolated from OSH, SH, LHMI and LH cells. Each lane contains 4 μg chlorophyll.

The mutant lacking the FRP (DF) and the mutant missing the Met26 (LHMI) recovered the lost fluorescence very slowly and even after 30 min incubation in dim light did not recover the full capacity of the antenna (Fig. 5A and S3). We have already shown that M26I mutation does not inactivate the long FRP. In consequence, the similar recovery phenotype observed in DF and LHMI cells could be explained only by the lack of the long FRP. This was confirmed by Western-blot analysis. The anti-FRP antibody was unable to detect any FRP in this mutant (Fig. 5B) We concluded that FRP begins at Met26 and not at Met1 when the *frp* gene is under its own promoter.

Fig. 5B also shows that the concentration of short FRP in OSH cells is largely higher than the concentration of short FRP in SH cells and most probably in WT cells. Thus, these results confirm that the low fluorescence quenching and rapid recovery observed in OSH cells is related to a high concentration of short FRP. The fact that the lost fluorescence recovered with similar kinetics in OLHMI and SH or WT cells (compared Figs. 3B with 5A), even though the concentration of FRP is largely higher in OLHMI cells confirmed that the long FRP has a much lower activity than the short FRP.

3.3. Influence of the presence of the His-tag on fluorescence quenching and OCP concentration

An unexpected result was observed when LHMI and SH *Synechocystis* mutant cells were illuminated with strong blue-green light (870 μmol photons m^{-2} s^{-1}) (Fig. 6). Strong blue-green light induced decrease of fluorescence in all the strains. However, while in WT and DF (lacking FRP) cells, Fm' decreased by 30–35%, in the other three strains containing a His-tag after Met1 (LH and LHMI) or Met26 (SH), Fm' decreased only by 15–20%. In addition, in the SH mutant, the kinetics of fluorescence quenching was slightly different. In all the other strains most of the fluorescence quenching occurred in the first minute of illumination. In contrast, in SH cells, the decrease of fluorescence was slower (Fig. 6).

The amount of fluorescence quenching is related to the concentration of OCP^r accumulated in the cells [15–17,22] and the mutants having less blue-green light induced fluorescence quenching are expected to accumulate a lower quantity of OCP^r. A decrease in OCP^r concentration could be due to a lower concentration of OCP or to a higher concentration or activity of FRP. In order to understand the cause of the lower fluorescence quenching in the three *frp* mutants containing an N-terminal His-Tag, Western-blot analysis was

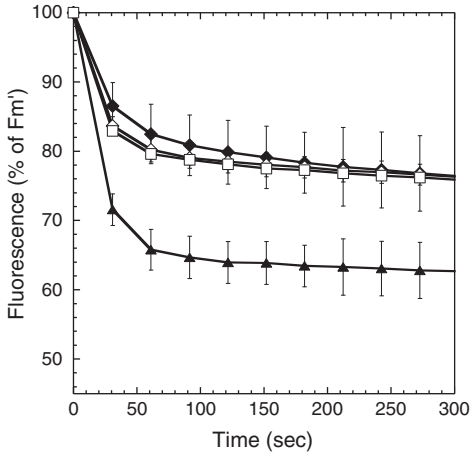

Fig. 6. Induction of the photoprotective mechanism in WT and FRP mutant *Synechocystis* cells. Decrease of maximal fluorescence (Fm') in WT (closed triangles), SH (closed rhomboids), LH (open rhomboids) and LHMI (open squares) cells during exposure to 870 μmol photons m^{-2} s^{-1} blue-green light at 30 °C. The cells were at a chlorophyll concentration of 3 μg/mL. Average of three independent measurements. Error bars represent SD.

undertaken to compare the amount of OCP in the cells. Fractions containing the phycobilisomes attached to the membranes (MP), in which all the OCP is present [10], were isolated from the three mutants and the WT. Their proteins were separated by SDS–PAGE and the OCP was detected by Western-blot using an anti-OCP antibody [23] (Fig. 7A). In mutant cells containing a His-tag downstream Met1 (LH or LHMI), the quantity of OCP in the MP was 50% lower than in the MP of WT (Fig. 7B). Thus, in these mutants the lower fluorescence quenching is explained by a lower concentration of OCP. In contrast, in the SH mutant, which contains a FRP with a His-tag after Met26 (SH), the concentration of OCP was similar to that in the WT. Therefore, most probably changes in FRP concentration or activity must cause the lower fluorescence quenching. This was also suggested by a slightly faster fluorescence recovery in the first minute of cell exposure to dim light (Fig. 5A). Unfortunately, since our antibody against FRP does not recognize the WT FRP [18], we cannot compare the concentration of FRP in SH cells to that in WT cells.

To try to understand why the introduction of 6 Histidines after Met1 decreased the concentration of OCP in the cells, we modeled the structures of potential RNA in-between the ORFs of OCP and short/long FRP (Fig. 8). The model described in the figure has the most negative ΔG value out of 4 structures generated for this sequence by an on-line tool mfold (http://mfold.rna.albany.edu/?q=mfold) [24]. Nevertheless, in the 4 proposed models, the sequence downstream FRP Met1 forms a stable hairpin. It is possible that this hairpin, together with the following polyT sequence forms a rho-independent transcription terminator of the *opc* gene. Introduction of a His-tag after Met1 results in destabilization of the hairpin, which could affect transcription termination giving a longer mRNA (Fig. 8). This longer mRNA which is likely less stable and more exposed to digestion by exonucleases due to the destabilized hairpin could be an explanation for the lower concentration of OCP in the LH and LHMI. This hypothesis must be confirmed.

4. Conclusions

The results obtained in this study allow us to state that the first Met of the *Synechocystis* FRP is the residue currently annotated as Met26. The long FRP (starting at Met1) The long FRP (starting at Met1) was present only when the long *frp* gene was under the control of the *psbA2* promoter. This longer protein was much less active than the short FRP and had a stronger interaction with the membrane. The short FRP is clearly a soluble protein like the OCP. We could speculate

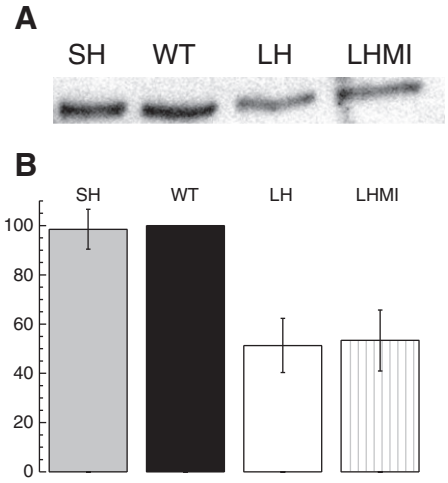

Fig. 7. OCP detection in membrane-phycobilisome preparation (MP) isolated from WT and FRP mutant cells. (A) Immunoblot detection of OCP in MP from SH, WT, LH and LHMI cells. Each well contained 0.05 μg chlorophyll. (B) Comparative densitometry of OCP bands in SH, WT, LH and LHMI MPs. Bars indicate relative concentration of OCP with 100% for WT. Average of three experiments with SD as the error bars.

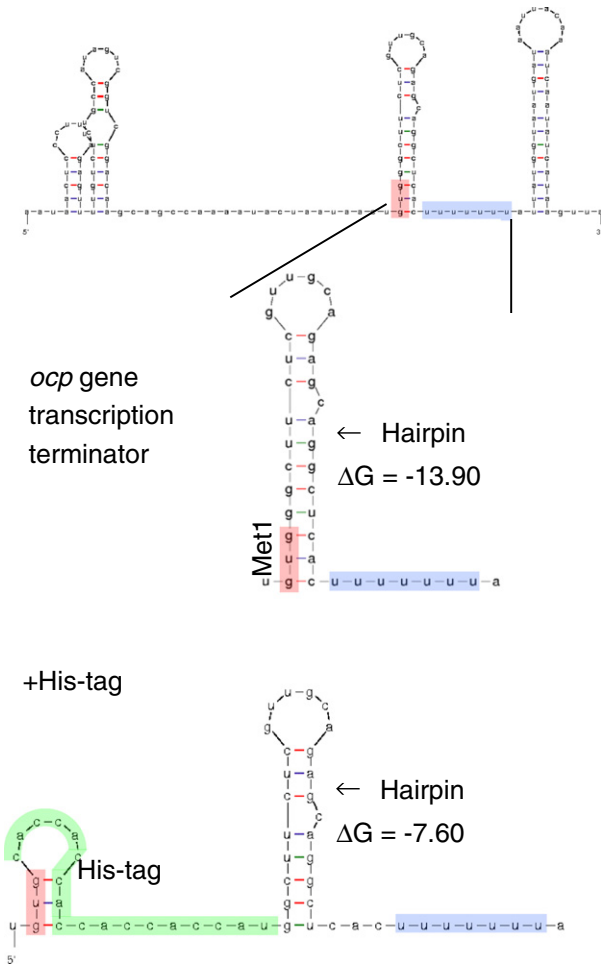

Fig. 8. A model of the RNA structure for the untranslated region between *ocp* and short-*frp* ORFs. Structures generated by mfold on-line tool. The presented structure (for complete region, upper) has the most negative ΔG (−35.4 kcal/mol) out of 4 structures proposed by mfold for this region at 37 °C. The FRP Met1 codon (gtg) is highlighted in red-transparent. Stable hairpin downstream the FRP Met1 with the poly-T region (highlighted in blue) forms the possible *ocp* transcription terminator (structure in the middle). In all 4 proposed structures the hairpin downstream the Met1 codon was destabilized by insertion of the his-tag (highlighted in green in the lower structure; mutants LH and LHMI) as indicated by the ΔG values for the hairpin (−13.9 and −7.6 kcal/mol hairpin alone in structures without or with his-tag, respectively).

that also in *Mycrocystis* NIES 843, a strain closely related to *Synechocystis*, the FRP does not have the N-terminal prolongation predicted by Cyanobase.org. In addition, transcription starting sites (TSS) were reported at the ATG coding for Met26 in *Synechocystis* and Met1 in *Anabaena* PC 7120 [25,26]. Based on these data, we can assume that *frp* is translated from a leaderless mRNA (not having 5′UTR) however, a longer *frp* mRNA containing at least 120 nucleotides upstream the first ATG of the short *frp* gene was previously detected in *Synechocystis* [18]. More specific studies about the promoter region of *frp* and its transcriptional regulation will give us further information about the transcription starting site and the cis and trans elements involved in the regulation.

Our results also indicate that the synthesis of OCP and FRP must be strictly regulated to obtain a high OCP to FRP ratio under conditions in which photoprotection is needed. A high FRP concentration inhibits photoprotection by destabilization of OCP^r. Thus, the amplitude of the OCP-related photoprotective mechanism could be regulated not only by the concentration of OCP but also by that of FRP. A high OCP to FRP ratio is necessary to induce photoprotection.

Acknowledgments

We thank Sandrine Cot for technical assistance. We thank Dr. Miguel Hernandez, Prof. Annegret Wilde for information and discussions about RNA TSPs. We thank Dr. Anja Krieger, Dr. Ghada Ajlani, Dr. Rocio Lopez Igual and Denis Jallet for critical reading of the manuscript. This research was supported by grants from the Agence Nationale de la Recherche (ANR, project CYANOPROTECT), the Centre National de la Recherche Scientifique (CNRS), the Commissariat à l'Energie Atomique (CEA) and HARVEST EU FP7 Marie Curie Research Training Network. MG is financed from the HARVEST ITN.

Appendix A. Supplementary data

Supplementary data to this article can be found online at http://dx.doi.org/10.1016/j.bbabio.2012.11.001.

References

[1] R. Croce, H. van Amerongen, Light-harvesting and structural organization of Photosystem II: from individual complexes to thylakoid membrane, J. Photochem. Photobiol. B 104 (2011) 142–153.
[2] A.V. Ruban, M.P. Johnson, C.D.P. Duffy, The photoprotective molecular switch in the photosystem II antenna, Biochim. Biophys. Acta 1817 (2012) 167–181.
[3] P. Jahns, A.R. Holzwarth, The role of the xanthophyll cycle and of lutein in photoprotection of photosystem II, Biochim. Biophys. Acta 1817 (2012) 182–193.
[4] A.N. Glazer, Phycobilisome-a macromolecular complex optimized for light energy transfer, Biochim. Biophys. Acta 768 (1984) 29–51.
[5] A.R. Grossman, M.R. Schaefer, G.G. Chiang, J.L. Collier, The phycobilisome, a light-harvesting complex responsive to environmental conditions, Microbiol. Rev. 57 (1993) 725–749.
[6] R. MacColl, Cyanobacterial phycobilisomes, J. Struct. Biol. 124 (1998) 311–334.
[7] N. Adir, Elucidation of the molecular structures of components of the phycobilisome: reconstructing a giant, Photosynth. Res. 85 (2005) 15–32.
[8] K. El Bissati, E. Delphin, N. Murata, A.-L. Etienne, D. Kirilovsky, Photosystem II fluorescence quenching in the cyanobacterium *Synechocystis* PCC 6803: involvement of two different mechanisms, Biochim. Biophys. Acta 1457 (2000) 229–242.
[9] M. Scott, C. McCollum, S. Vasil'ev, C. Crozier, G.S. Espie, M. Krol, N.P.A. Huner, D. Bruce, Mechanism of the down regulation of photosynthesis by blue light in the Cyanobacterium *Synechocystis* sp PCC 6803, Biochemistry 45 (2006) 8952–8958.
[10] A. Wilson, G. Ajlani, J. Verbavatz, I. Vass, C. Kerfeld, D. Kirilovsky, A soluble carotenoid protein involved in phycobilisome-related energy dissipation in cyanobacteria, Plant Cell 18 (2006) 992–1007.
[11] N. Karapetyan, Non-photochemical quenching of fluorescence in cyanobacteria, Biochemistry (Mosc.) 72 (2007) 1127–1135.
[12] C. Kerfeld, M. Sawaya, V. Brahmandam, D. Cascio, K. Ho, C. Trevithick-Sutton, D. Krogmann, T. Yeates, The crystal structure of a cyanobacterial water-soluble carotenoid binding protein, Structure 11 (2003) 55–65.
[13] C. Kerfeld, Structure and function of the water-soluble carotenoid-binding proteins of cyanobacteria, Photosynth. Res. 81 (2004) 215–225.
[14] C.A. Kerfeld, Water-soluble carotenoid proteins of cyanobacteria, Arch. Biochem. Biophys. 430 (2004) 2–9.
[15] A. Wilson, C. Punginelli, A. Gall, C. Bonetti, M. Alexandre, J. Routaboul, C. Kerfeld, R. van Grondelle, B. Robert, J. Kennis, D. Kirilovsky, A photoactive carotenoid protein acting as light intensity sensor, Proc. Natl. Acad. Sci. U. S. A. 105 (2008) 12075–12080.
[16] C. Punginelli, A. Wilson, J. Routaboul, D. Kirilovsky, Influence of zeaxanthin and echinenone binding on the activity of the Orange Carotenoid Protein, Biochim. Biophys. Acta 1787 (2009) 280–288.
[17] M. Gwizdala, A. Wilson, D. Kirilovsky, In Vitro reconstitution of the cyanobacterial photoprotective mechanism mediated by the orange carotenoid protein in *Synechocystis* PCC 6803, Plant Cell 23 (2011) 2631–2643.
[18] C. Boulay, A. Wilson, S. D'Haene, D. Kirilovsky, Identification of a protein required for recovery of full antenna capacity in OCP-related photoprotective mechanism in cyanobacteria, Proc. Natl. Acad. Sci. U. S. A. 107 (2010) 11620–11625.
[19] T. Liu, Y. Shuai, H. Zhou, Purification, crystallization and preliminary X-ray diffraction of fluorescence recovery protein from *Synechocystis* PCC 6803, Acta Crystallogr. F Struct. Biol. Cryst. Commun. 67 (2011) 1627–1629.
[20] A. Wilson, C. Punginelli, M. Couturier, F. Perreau, D. Kirilovsky, Essential role of two tyrosines and two tryptophans on the photoprotection activity of the Orange Carotenoid Protein, Biochim. Biophys. Acta 1807 (2011) 293–301.
[21] Y. Kashino, H. Koike, K. Satoh, An improved sodium dodecyl sulfate-polyacrylamide gel electrophoresis system for the analysis of membrane protein complexes, Electrophoresis 22 (2001) 1004–1007.
[22] A. Wilson, M. Gwizdala, A. Mezzetti, M. Alexandre, C.A. Kerfeld, D. Kirilovsky, The essential role of the N-terminal domain of the orange carotenoid protein in cyanobacterial photoprotection: importance of a positive charge for phycobilisome binding, Plant Cell 24 (2012) 1972–1983.
[23] A. Wilson, C. Boulay, A. Wilde, C.A. Kerfeld, D. Kirilovsky, Light-induced energy dissipation in iron-starved cyanobacteria: roles of OCP and IsiA proteins, Plant Cell 19 (2007) 656–672.
[24] M. Zuker, Mfold web server for nucleic acid folding and hybridization prediction, Nucleic Acids Res. 31 (2003) 3406–3415.
[25] J. Mitschke, J. Georg, I. Scholz, C.M. Sharma, D. Dienst, J. Bantscheff, B. Voss, C. Steglich, A. Wilde, J. Vogel, W.R. Hess, An experimentally anchored map of transcriptional start sites in the model cyanobacterium *Synechocystis* sp PCC6803, Proc. Natl. Acad. Sci. U. S. A. 108 (2011) 2124–2129.
[26] J. Mitschke, A. Vioque, F. Haas, W.R. Hess, A.M. Muro-Pastor, From the cover: dynamics of transcriptional start site selection during nitrogen stress-induced cell differentiation in *Anabaena* sp PCC7120, Proc. Natl. Acad. Sci. U. S. A. 108 (2011) 20130–20135.